Orientation of Hot-Drawn Poly(butylene terephthalate) Films As Determined from the Intrinsic Polarized Fluorescence†

Manfred Hennecke*

Federal Institute for Materials Research and Testing, Unter den Eichen 87, D-1000 Berlin 45, FRG

Klaus Kurz and Jürgen Fuhrmann

Institut für Physikalische Chemie, TU Clausthal, P.O.B. 1252, D-3392 Clausthal-Zellerfeld, FRG

Received August 14, 1991; Revised Manuscript Received July 9, 1992

ABSTRACT: As far as indicated by the spectra and the fluorescence time decay law, the properties of the fluorescence of poly(butylene terephthalate) (PBT) are almost identical to those of PET. The ground-state-stable sandwich dimers in the noncrystalline regions of uniaxially-drawn PBT films were used as chain-intrinsic fluorescent labels for studying the orientation distribution function. The dimers are formed only in the amorphous regions; concerning the fluorescence signal, "amorphous" includes all the material outside perfect crystallites. During deformation, the orientation coefficient $\langle P_2 \rangle^F$ of the dimers follows approximately a superposition curve of crystallite-like orientation, easily separable in the initial range of stretching ratio $\lambda < 2.5$, and of true-amorphous orientation of the affine network type that becomes noticeable at $\lambda > 3$. The total fluorescence intensity of PBT, if excited at the proper wavelength, is proportional to the concentration of the dimers; it remains constant in the initial range of stretching, i.e. $\lambda < 1.5$. At higher λ, correlated to the increase of amorphous orientation, a strong increase of the dimer concentration, up to a factor of 6, is observed.

Introduction

Among the aromatic polyesters derived from terephthalic acid, poly(ethylene terephthalate) (PET) and poly(butylene terephthalate) (PBT) have the most important applications as engineering plastics. In order to increase the orientational order, and thus improve the mechanical properties, deformation is a necessary step in polyester technology. In numerous studies the orientation and deformation process during uni- or biaxial stretching of PET and PBT films has been investigated.[1-4]

Recently,[5,6] it has been shown, by means of polarized fluorescence measurements of PET films, that the bimolecular ground-state-stable association of PET (named "dimer" in what follows) can be used as a chain-intrinsic fluorescent label for studying the orientation in the noncrystalline regions where the dimers are exclusively formed. Essential results were confirmed by other authors.[7,8] The assignment of the discussed component of the PET fluorescence to noncrystalline regions is based upon the following arguments. By excitation with a wavelength of $\lambda_{exc} = 340$ nm, absorption of the monomer, i.e. the terephthalic acid ester, cannot occur; the monomer absorbs at 320 nm and below, giving rise to monomer fluorescence around 350 nm. This monomer fluorescence (sometimes accompanied by excimer fluorescence) was observed in solutions and in the solid state of PET, as well as in solutions and crystals of dimethyl terephthalate (DMT).[7,8] Inspection of the crystal structure of DMT,[9] PET,[10] and PBT[11] shows that in the respective unit cells the terephthalate groups are aligned in a stock manner with a separation of 0.4–0.5 nm. These distances are well beyond the value of about 0.35 nm which is needed for ground-state or exited-state interaction of benzene rings[12,13] to cause either a new intermolecular absorption band or an excimer, respectively. Contrary to the fixed separation in the crystal, the distribution of interchromophore distances in the frozen amorphous state can include, though rarely, face-to-face geometries of terephthalate units with the required small separation.[14] The assignment of the PET fluorescence ($\lambda_{exc} = 340$ nm, $\lambda_{flu} = 390$ nm) to a ground-state-stable dimer was further substantiated by fluorescence polarization measurements[5] and by the observation that the total fluorescence intensity increases during stretching of a PET film, without change of the spectral distribution. This occurs in a stretching range where the crystallites and their orientation are unaffected.[6]

The orientation of the dimer is characterized by the first two expansion coefficients $\langle P_2 \rangle^F$ and $\langle P_4 \rangle^F$ (F indicates fluorescence) of the orientation distribution function (odf) in Legendre polynomials, assuming rotational (uniaxial) symmetry of both the polymer matrix and the dimer fluorophore. During stretching, the orientation behavior can approximately be modeled by a superposition of crystallite-like (similar affine vector[1]) and true amorphous (affine network) orientation.[6]

In the case of PBT, the interest in uniaxial deformation has mostly been focused on the crystalline-phase transformation (α- and β-forms)[11,15,16] but less on the molecular orientation in the noncrystalline regions.[17]

Since isotropic PBT films show similar polarized fluorescence spectra and time decay laws in comparison with PET, we also postulate the existence of ground-state-stable dimers in the noncrystalline regions. As in PET, the crystallographic unit cells of α-PBT and β-PBT[11] do not allow the formation of dimers in the crystalline phase. In this article, the determination of the orientation coefficients by use of the intrinsic dimer fluorescence will be performed in the same way as with PET. Furthermore, a comparison of the orientation and deformation behavior between PET and PBT films, both uniaxially stretched above the glass transition temperature T_g, is made and discussed in terms of the above mentioned two-phase superposition model.

Experimental Section

The starting material for all experiments was a nearly isotropic ($\Delta n < 0.0005$) PBT film of 220-μm thickness supplied, additive

† Dedicated to H. G. Zachmann on the occasion of his 60th birthday.

0024-9297/92/2225-6190$03.00/0

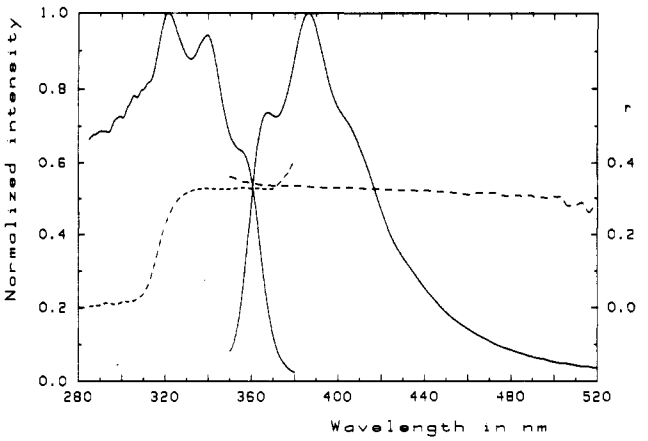

Figure 1. Normalized polarized excitation and fluorescence spectra of isotropic PBT at room temperature (film thickness 220 μm, slit width 2 nm, room temperature). The fluorescence wavelength of the excitation spectrum was λ_{flu} = 386 nm, and the excitation wavelength of the fluorescence spectrum was λ_{exc} = 338 nm. Broken curves: degree of polarization r (eq 2) of both spectra, right-side ordinate.

free, by Kalle AG, Wiesbaden, FRG. The degree of crystallinity, as determined by DSC was α = 0.33 and the glass transition temperature T_g = 346 K. The film was oriented by drawing strips of initially 20 mm wide and 30 mm long in a tension machine at a constant temperature of 351 K and at a constant strain rate v = 0.15%/s. PET samples were described earlier.[5,6]

Corrected polarized excitation and fluorescence spectra were obtained by means of a Perkin-Elmer MPF 44 spectrofluorometer specially equipped for polarized fluorescence measurements of solid samples.[5,6,18] The normalized total fluorescence intensity I and the degree of fluorescence polarization r (sometimes called emission anisotropy) were calculated according to eqs 1 and 2. Both quantities, I and r

$$I = I_{VV} + 2I_{VH} \tag{1}$$

$$r = \frac{I_{VV} - I_{VH}}{I_{VV} + 2I_{VH}} \tag{2}$$

were corrected for the instrumental spectral and polarization sensitivity by the method described[18,19] and were plotted against the wavelength. V and H denote the vertical and horizontal positions of the polarizers in the excitation (first subscript) and the fluorescence (second subscript) beam. In the case of an isotropic sample with diluted, immobile fluorophores, $r = r_0$, where r_0 is the fundamental polarization of the fluorophore.[18,19]

The polarized fluorescence intensities of the anisotropic specimens were measured during stretching and evaluated with the computer-controlled apparatus previously described.[6]

Fluorescence time decay laws were determined by means of a flash-lamp apparatus based on the "single photon counting technique".[6,20]

Results and Discussion

(a) Spectra, Polarization, and Fluorescence Time Decay. Figure 1 shows the polarized excitation and fluorescence spectra of an isotropic PBT film recorded at the maximum of fluorescence and excitation, respectively. By comparison of the spectra with those of isotropic PET[5,6] no significant differences in the wavelengths of the band maxima of excitation and fluorescence are noticed. The total intensity of the fluorescence of the used PBT film is clearly higher than the intensity of a PET film of equal thickness and crystallinity. For the dimer fluorescence of PBT, at λ_{exc} = 338 nm, an intensification of 1.5 is found; at λ_{exc} = 290 nm the intensity of PBT is only 1.2 times higher.

The spectral course of the degree of polarization r in Figure 1 is very similar to the corresponding behavior of

Table I
Parameters of the Biexponential Fluorescence Decay Law $I = \alpha_1 \exp(-t/\tau_1) + \alpha_2 \exp(-t/\tau_2)$ of PBT Films Measured at Room Temperature[a]

	isotropic film			oriented film					
				VVV[b]			VHV[b,c]		
λ_{exc}/nm	α_i/%	τ_i/ns	χ^2	α_i/%	τ_i/ns	χ^2	α_i/%	τ_i/ns	χ^2
338	98.4	1.1	1.2	99.0	1.0	1.1	99.5	1.1	1.2
	1.6	7.0		1.0	5.4		0.5	9.2	
290	79.1	3.6	1.0	89.2	3.7	1.2[c,d]			
	20.9	7.5		10.8	13.8				

[a] Wavelength of fluorescence λ_{flu} > 389 nm (edge filter). Stretching parameters of the oriented film: ratio λ = 5, T = 358 K, v = 5%/s. The quality of the fit is indicated by χ^2. Errors: τ_1 ±0.2 ns, τ_2 ±0.9 ns; $\alpha_{1,2}$ ±0.5%. [b] Setup VVV, polarizer, stretching axis, and analyzer vertical; VHV, stretching axis horizontal. [c] Errors: τ_1 ±0.2 ns, τ_2 ±3 ns; $\alpha_{1,2}$ ±2%; large errors due to very low intensity. [d] Measured without polarizers because of low intensity.

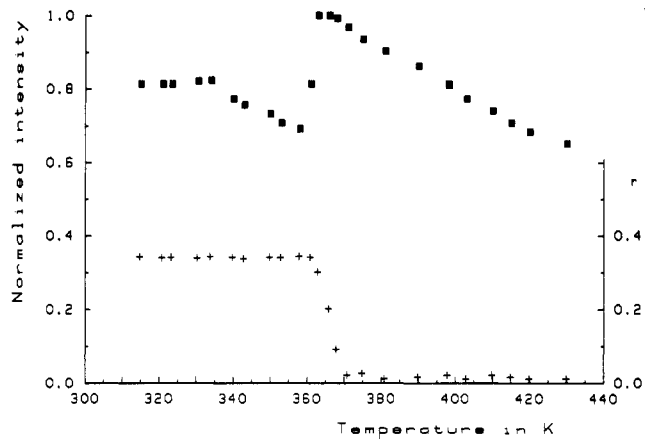

Figure 2. Total fluorescence intensity (eq 1) and degree of polarization (eq 2) of the used isotropic PBT film versus temperature: (■) intensity; (+) degree of polarization (right-side ordinate). λ_{exc} = 338 nm, λ_{flu} = 388 nm.

PET in the excitation and the fluorescence spectrum. The elevated plateau value of r ≈ 0.33 is achieved at λ_{exc} > 330 nm with λ_{flu} = 386 nm. The increase of r at the end of both spectra if approaching λ_{flu} and λ_{exc}, respectively, is due to (linearly polarized) scattered light from the exciting beam.

It was also verified that the spectra of stretched PBT films coincide with those of the isotropic film, apart from the spectral course of r which reflects the molecular orientation. The same coincidence was found in the case of PET[6]. The fluorescence time decay law of the dimer is also similar to that of PET[6] and independent of the selected polarized component (cf. Table I). It should be noted that, at λ_{exc} = 338 nm, the second fluorescent component contributes little to the fluorescence; essentially, there is a fast monoexponential fluorescence decay. At λ_{exc} = 290 nm a more distinct biexponential decay law is found; for this excitation wavelength where monomer and excimer, but no dimer, fluorescence is observed, the parameters of the time decay law change considerably with respect to the dimer. As indicated by the parameters of the stretched film, there exists also a dependence on the molecular orientation of the PBT film.

(b) Effect of Secondary Crystallization. During annealing of the used PBT above T_g, secondary crystallization occurs and at lower temperatures than in PET.[21] The onset of crystallization at 360 K is indicated by a strong enhancement of light scattering. This leads to an apparent increase of the fluorescence intensity which is mainly caused by the increase of the excited volume inside

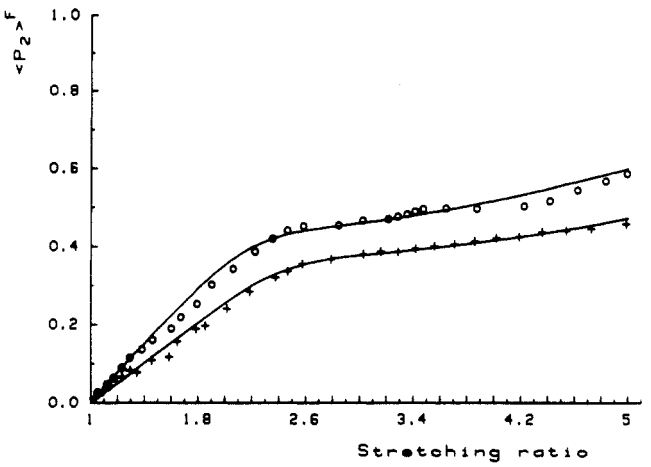

Figure 3. Orientation coefficient $\langle P_2 \rangle^F$ of PBT (+) and PET (O) dimers measured during stretching, plotted against the stretching ratio λ (stretching temperatures $T_g + 5$ K, rate 0.15%/s). Continuous lines: two-state model curves, superposition of crystallite orientation (weight: 37% for PBT, 44% for PET) and affine network orientation (required number of statistical segments: 30 for PBT, 20 for PET).

the specimen (Figure 2). Associated with the scattering power of the PBT film, especially in the UV range, is its ability to depolarize linearly polarized light; hence, above 370 K, the fluorescence of the turbid PBT film is almost completely depolarized. Near the glass transition temperature, at $T = 335$ K, a break in the intensity versus temperature curve, but not in the degree of polarization, is observed.

The measured temperature behavior of the polarized fluorescence of PBT is very similar to that of PET.[5] The only difference originates from the higher rate of crystallization at lower temperatures in PBT.[21] The crystallization-induced depolarization sets an upper limit of the temperature range wherein polarized fluorescence measurements can be evaluated. If homogeneously deformed samples are required, the lower limit of stretching temperature is given by T_g; hence, the temperature window lies between T_g and $T_g + 15$ K.

(c) Orientation Coefficient $\langle P_2 \rangle^F$ of PBT during Stretching. As mentioned above, the spectral and time-resolved parameters of the dimer fluorescence of PBT are essentially independent of the orientation of the film. Hence, the polarized intensities can be used to characterize the stretch-induced changes of the orientation of the polymer chains. In the case of fiber symmetry, the odf, characterized by $\langle P_2 \rangle^F$ and $\langle P_4 \rangle^F$, depends only on the angle β between the molecular chain axis and the stretching direction. Since dimers cannot exist in the perfect crystal, the fluorescence polarization signal is confined to the orientation of the amorphous regions. $\langle P_2 \rangle^F$ can be factorized

$$\langle P_2 \rangle^F = \langle P_2 \rangle^\sigma \langle P_2 \rangle^A \qquad (3)$$

where $\langle P_2 \rangle^\sigma$ indicates the correlation between the dimer orientation and the orientation coefficient $\langle P_2 \rangle^A$ of the amorphous regions. With PET, a value of $\langle P_2 \rangle^\sigma \approx 0.90$ was determined,[6] the linear relationsship being valid in the whole range of realized $\langle P_2 \rangle^F$, i.e. 0–0.7. The value of $\langle P_2 \rangle^\sigma$ close to 1 signifies the strong correlation and gives additional support to the conclusion that the chromophores are part of the polymer chain.

Figure 3 shows the development of $\langle P_2 \rangle^F$ as a function of the stretching ratio λ and allows a comparison to the behavior of a PET film which was stretched at the same temperature $T_g + 5$ K and at the same stretching rate. The $\langle P_2 \rangle^F$ curves of both polymers show qualitatively the same features. In the range $1 \le \lambda \le 2.5$ where the alignment of crystallites to the stretching direction evolves, a strong, and nearly linear, increase of $\langle P_2 \rangle^F$ occurs. Above $\lambda = 2.5$, the orientation of the crystallites has almost finished and the subsequent increase of $\langle P_2 \rangle^F$ is prevailingly due to the chain orientation in the amorphous regions. Since fluorescent dimers can only be formed in the amorphous regions, it is self-suggesting to describe the course of $\langle P_2 \rangle^F$ and hence the amorphous orientation by a two-state model:[6] one part of the amorphous phase is oriented simultaneously with, and to the same extent as, the crystallites whilst the other part orients like network chains with the crystallites acting as network junctions. The course of the orientation coefficients in Figure 3 can be satisfactorily fitted by the superposed, and properly weighted, model curves (for a graphical representation see ref 6). The percentage of the amorphous phase that is oriented like crystallites (sometimes called the rigid-amorphous fraction) is 37% for PBT and 44% for PET, respectively. To obtain the best fit, the required mean number of statistical network segments for the "true-amorphous" part is 30 for PBT and 20 for PET.

Concerning the determination of $\langle P_2 \rangle^\sigma$ (eq 3), it was found that the linearity of the plot of $\langle P_2 \rangle^F$ versus birefringence was insufficient in the available range of data to allow a precise statement. Nevertheless, the possible range of $\langle P_2 \rangle^\sigma$ lies between 0.7 and 1; this range includes the value of PET, i.e. $\langle P_2 \rangle^\sigma \approx 0.90$, and indicates strong correlation between dimer and amorphous orientation. Therefore, the $\langle P_2 \rangle^F$ data have been taken for the evaluation of the model parameters without correction for $\langle P_2 \rangle^\sigma$.

In view of the higher flexibility of the PBT chain with respect to PET, the differences in both parameters (the percentage of crystallite-like orientation and the number of network segments) which lead to reduced values of $\langle P_2 \rangle^F$ are quite understandable.

(d) Type of the Orientation Distribution Function. From the values of $\langle P_4 \rangle^F$ at a given $\langle P_2 \rangle^F$ a certain characterization of the type of the orientation distribution function can be made. Within the limits of experimental accuracy, the $\langle P_4 \rangle^F$ data at $\lambda < 2$ are close to zero and agree with the affine vector model of orientation[1] which describes the preferred orientation of rigid rods or revolution ellipsoids in an affinely deformed matrix.

For stretching ratios $\lambda > 2$, and orientation values $\langle P_2 \rangle^F > 0.3$, there is a tendency of $\langle P_4 \rangle^F$ to spread systematically below the affine curve; with stretching temperatures close to T_g, even small negative numbers of $\langle P_4 \rangle$ were obtained.

The same behavior was noticed, though less marked, with PET,[6] and it means that the maximum of the odf does not lie at the stretching direction but at some angle with respect to it.

(e) Fluorescence Intensity during Stretching. As shown in Figure 4, the normalized total fluorescence intensity (versus stretching ratio) remains approximately constant up to $\lambda = 1.5$, or $\langle P_2 \rangle^F = 0.1$. Subsequently, a strong increase to 400% of the initial value at $\lambda = 1$ is observed; with samples stretched close to T_g, the increase achieves even 600%. The plotted values of intensity in Figure 4 are corrected for the thickness t of the film; hence, I/t (see eq 1) is shown. We assume that the absorption coefficient and the quantum yield of the fluorescence remain constant during stretching; then the increase of intensity reflects the formation of dimer chromophores, associated with the improved alignment in the true-amorphous regions. From Figure 5 the relationship

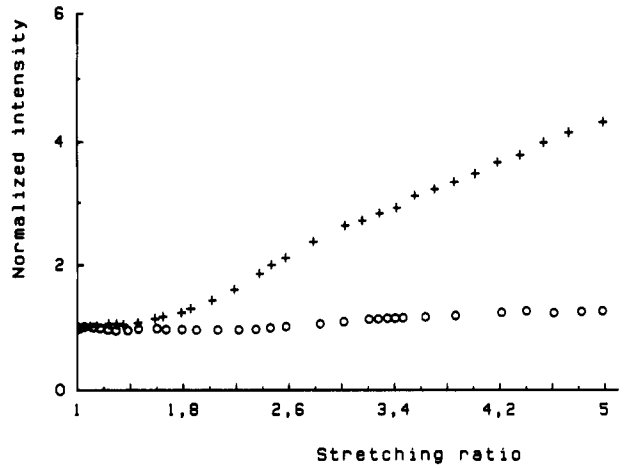

Figure 4. Normalized total fluorescence intensity I/t (divided by the thickness t of the film) of PBT (+) and PET (O), measured during stretching, plotted against the stretching ratio. For experimental conditions see Figure 3.

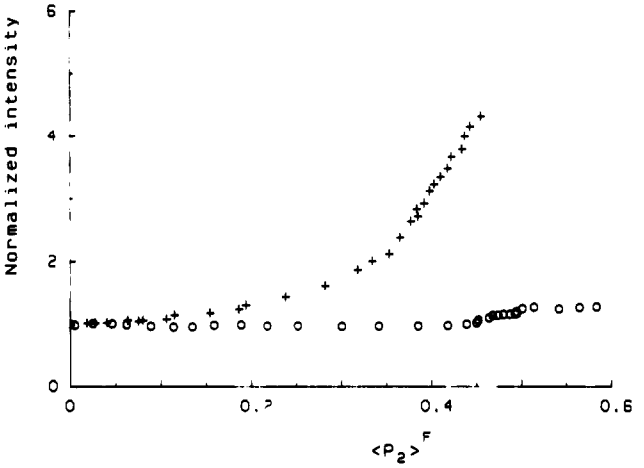

Figure 5. Total fluorescence intensity (I/t (see Figure 4), plotted against the orientation coefficient $\langle P_2\rangle^F$ of the dimers. For experimental conditions see Figure 3.

between fluorescence intensity and orientation coefficient $\langle P_2\rangle^F$ can be gathered in more detail. A strong increase of intensity occurs above $\langle P_2\rangle^F = 0.35$ in the case of PBT. At this state of the stretched sample, the orientation of the crystallites and hence the orientation of the rigid-amorphous fraction has finished. Therefore, subsequent improvement of dimer orientation can take place only in the true-amorphous regions. Whereas the dimer orientation reflects the chain orientation with respect to the stretching axis (cf. section c), eq 3, the probability of dimer formation is expected to depend on the parallelism of terephthalic groups (but not on their orientation to the stretching axis). Such a mutual chain orientation is described by the pair orientation coefficient $\langle {}^2P_2\rangle$ (the superscript 2 denotes that it belongs to the pair odf). The stretch-induced mechanism of orientation that acts by rotation of the principal axis of large anisotropic areas into the direction of stretching is not accompanied by an increase of $\langle {}^2P_2\rangle$; this mechanism is dominant for the rigid-amorphous fraction around the crystallites. On the other hand, within an orientation gas model,[22] the relationship between $\langle {}^2P_2\rangle$ and $\langle P_2\rangle$ of a homogeneously deformed specimen is simply given by

$$\langle {}^2P_2\rangle = (\langle P_2\rangle)^2 \quad (4)$$

Such an orientation mechanism may be dominant in the true-amorphous fraction. Obviously, the course of intensity versus $\langle P_2\rangle^F$ in Figure 5 shows some similarity to parabolic behavior, but the type of the correlation between the number of dimer fluorophores and the pair orientation coefficient can only be proved if $\langle {}^2P_2\rangle$ would be known in the stretched PBT.

The formation of additional fluorophores clearly overwrites the contradictory effect which is the volume loss of the amorphous fraction caused by stress-induced crystallization. In the case of PET, evidence for this influence may be drawn from the intensity behavior up to $\langle P_2\rangle^F = 0.5$ where a small decrease of the total fluorescence intensity is found. As can be seen from Figures 4 and 5, the change of the dimer concentration in PET that occurs during stretching is less pronounced.

Concerning the fluorescence intensity, we argue that the difference between PBT and PET comes from the larger true-amorphous fraction in the case of PBT. In addition, the higher flexibility of the polymer chain facilitates, in the case of PBT, the necessary alignment of the aromatic groups to form dimers.

Conclusions

The fluorescence spectrum, the degree of polarization, and the time decay law of the fluorescence in isotropic and anisotropic PBT films are very similar to the corresponding properties of PET. We conclude that the fluorophore of PBT is the ground-state stable dimer of the terephthalic group which can be used as a suitable label of the chain orientation in the same way as in PET. The orientation coefficients $\langle P_2\rangle^F$ and $\langle P_4\rangle^F$ can be interpreted as a direct measure of the orientation in the noncrystalline regions of PBT.

The behavior of $\langle P_2\rangle^F$ and $\langle P_4\rangle^F$ during stretching follows approximately a superposition of two orientation models, one for the crystallite-like fraction (similar affine vector) and the other for the true-amorphous fraction (affine network).

The differences in the polarized fluorescence properties between PBT and PET, particularly concerning the formation of dimers during stretching, reflect the different flexibility of the polyester chains. The formation of dimer fluorophores during stretching may be taken as a sensitive tool for mutual chain alignment in the true-amorphous regions; it may even be an indicator of the existence of such regions.

Acknowledgment. This work was granted by the Deutsche Forschungsgemeinschaft. K.K. acknowledges a thesis grant from the federal state of Rheinland-Pfalz.

References and Notes

(1) Ward, I. M. *Structure and Properties of Oriented Polymers*; Applied Science Ltd.: London, 1975.
(2) Thistlethwaite, T.; Jakeways, R.; Ward, I. M. *Polymer* **1988**, *29*, 61.
(3) Zachmann, H. G. *Polym. Eng. Sci.* **1979**, *19*, 966.
(4) Song, J. W.; Abhiraman, A. S.; Rickards, A. P. *J. Appl. Polym. Sci.* **1982**, *27*, 2369.
(5) Hennecke, M.; Fuhrmann, J. *Makromol. Chem. Macrom. Symp.* **1986**, *5*, 181.
(6) Hennecke, M.; Kud, A.; Kurz, K.; Fuhrmann, J. *Colloid Polym. Sci.* **1987**, *265*, 674.
(7) Hemker, D. J.; Thomas, J. W.; Frank, C. W. *Polymer* **1988**, *29*, 437.
(8) Sonnenschein, M. F.; Roland, M. *Polymer* **1990**, *31*, 2023.
(9) Orsa, A. ASTM Powder Diffraction Data Card No. 11-713, 1960.
(10) Daubeny, R. de P.; Bunn, C. W.; Brown, C. J. *Proc. R. Soc. London* **1954**, *A226*, 531.
(11) Stambaugh, B.; Koenig, J. L.; Lando, J. B. *J. Polym. Sci. Polym. Phys. Ed.* **1979**, *17*, 1053.
(12) Birks, J. B. *Organic Molecular Photophysics*; J. Wiley & Sons: London, 1975.
(13) Phillips, D. H.; Schug, J. C. *J. Chem. Phys.* **1969**, *10*, 3297.

(14) Cao, T.; Magonov, S. N.; Qian, R. *Polym. Commun.* **1988**, *29*, 431.
(15) Stein, R. S.; Misra, A. *J. Polym. Sci. Polym. Phys. Ed.* **1980**, *18*, 327.
(16) Siesler, H. W. *Adv. Polym. Sci.* **1984**, *65*, 1.
(17) Strohmeier, W.; Frank, W. F. *Colloid Polym. Sci.* **1982**, *260*, 937.
(18) Hennecke, M. Habilitationsschrift, TU Clausthal, 1989.
(19) Lakowicz, J. R. *Principles of Fluorescence Spectroscopy*; Plenum Press: New York, 1983.
(20) Ware, W. R. In *Creation and Detection of the Excited State*; Lamola, A. A., Ed.; M. Dekker: New York, 1978; Vol. 1A, Chapter 5.
(21) Gilbert, M.; Hybart, F. J. *Polymer* **1974**, *15*, 407.
(22) Zannoni, C. In *The Molecular Physics of Liquid Crystals*; Luckhurst, G. R., Gray, G. W., Eds.; Academic Press: London, 1979; Chapter 3.

Registry No. PBT (SRU), 24968-12-5; PBT (copolymer), 26062-94-2.